
Figures and figure supplements

Wnt, Ptk7, and FGFR1 expression gradients control trunk positional identity in planarian regeneration

Rachel Lander and Christian P Petersen

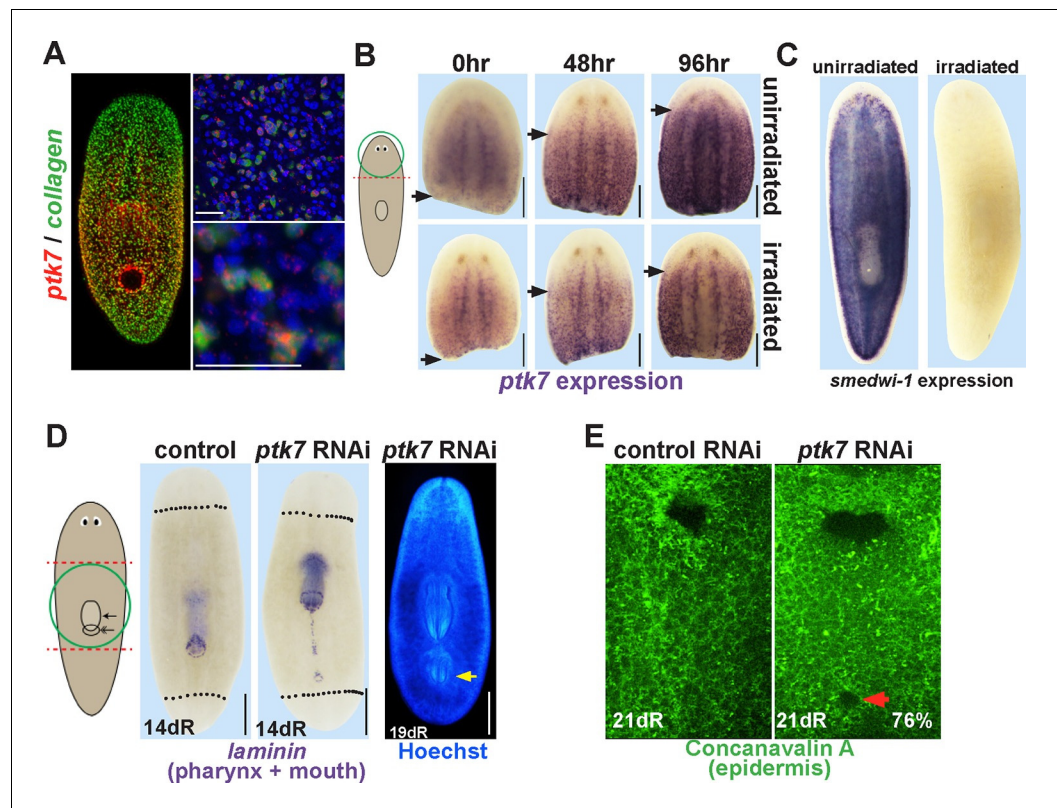


Figure 1. *ptk7* is a positional control gene that suppresses trunk identity in regenerating planarians. (A) Left panel, Double FISH to detect coexpression of *ptk7* within *collagen*⁺ cells of the body-wall musculature in a trunk-centered gradient (116/125 *collagen*⁺ cells were *ptk7*⁺ and 113/125 *ptk7*⁺ cells were *collagen*⁺, scored in ventral prepharyngeal subepidermal region). Right panels, higher magnification of *collagen*⁺*ptk7*⁺ cells. (B, upper panels) Freshly amputated head fragments have *ptk7* expression in the CNS but minimal levels in subepidermal cells but by 48–96 hr expression appears at a region within the new anterior of the fragment (arrows, anterior extent of *ptk7* expression). (B, lower panels) Animals treated with lethal doses of gamma irradiation (6000 Rads) three days prior to amputation undergo a similar re-establishment of a *ptk7* expression domain along the A-P axis. Images represent at least 3/3 animals probed. (C) Irradiation controls showing elimination of *smedwi-1*-expressing neoblasts in animals from the same cohort as (B). (D) Animals were injected with control or *ptk7* dsRNA three times over three days, amputated to remove heads and tails, allowed to regenerate, fixed at 14 days and stained with a *laminin* riboprobe detecting both the mouth and pharynx (left panels, dotted line indicates amputation plane, red box shows enlarged region of *ptk7*(RNAi) animals) or stained with Hoechst dye to label nuclei and visualize the pharynx (right). *ptk7* RNAi caused formation of an ectopic posterior mouth in regenerating trunk fragments (28/35 animals), but not in regenerating head or tail fragments (35/35 animals each). (D, right) More rarely, *ptk7* inhibition caused formation of an ectopic posterior pharynx. (E) Control or *ptk7*(RNAi) animals stained with a fluorescent lectin Concanavalin A to visualize the epidermis and the pre-existing or ectopic mouth (red arrow). Bars, 25 (A), or 200 (B), or 400 microns (D–E).

DOI: [10.7554/eLife.12850.003](https://doi.org/10.7554/eLife.12850.003)

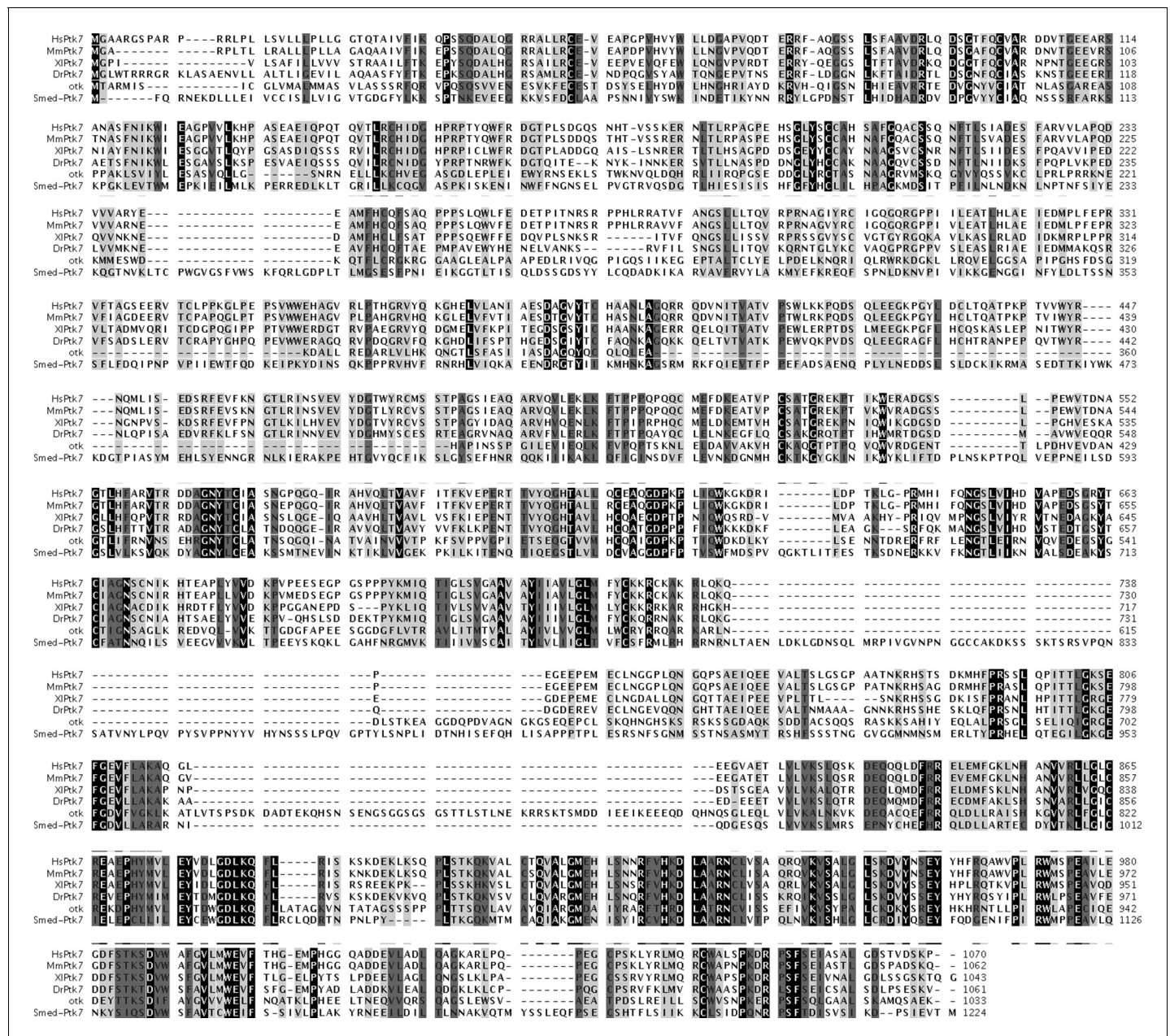


Figure 1—figure supplement 1. Sequence alignment of *Smed-ptk7*. Alignment of predicted protein sequence of *Smed-ptk7* with human (HsPtk7, NP_002812.2), mouse (MmPtk7, AAH76578.1), *Xenopus laevis* (XlPtk7, NP_001083315.1), zebrafish (DrPtk7, AGT63300.1) and *Drosophila melanogaster* (otk, AAF58596.1) Ptk7 proteins. SMED-PTK7 is predicted to have 7 extracellular Ig-family domains and an intracellular tyrosine kinase domain (<http://smart.embl-heidelberg.de>).

DOI: 10.7554/eLife.12850.004

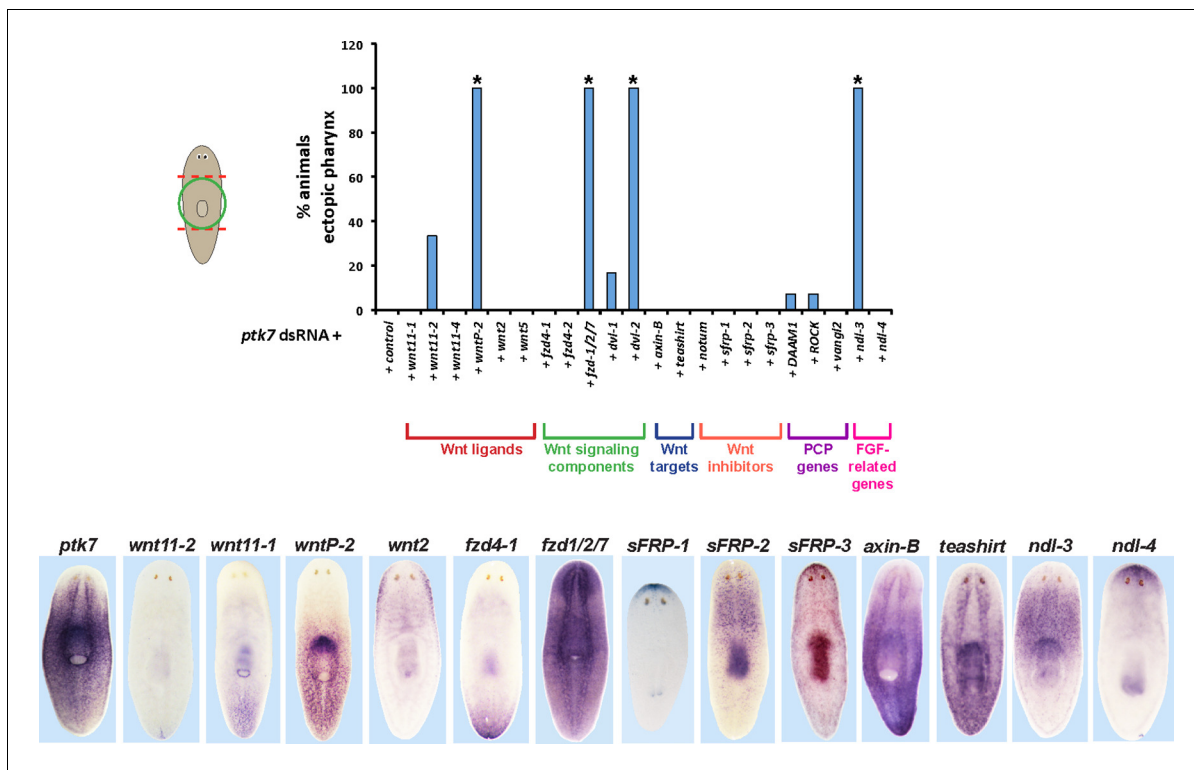


Figure 1—figure supplement 2. RNAi enhancement screen identifies modulators of *ptk7* activity involved in trunk patterning. (Upper) Plot of ectopic posterior pharynx phenotype penetrance after administration of dsRNA targeting *ptk7* and each of 22 previously identified positional control genes or Wnt-related factors expressed regionally along the body axis (*wnt11-1*, *wnt11-2*, *wnt11-4*, *wntP-2*, *wnt2-1*, and *wnt5*), general intracellular components of Wnt signaling (frizzled receptors expressed in the posterior: *fzd4-1/fzd4*, *fzd4-2*, and *fzd1/2/7*; Disheveled proteins: *Dvl-1* and *Dvl-2*), downstream components of Wnt signaling that act positively (*teashirt*) or negatively (*axin-B*) to influence β -catenin-1 signaling, secreted Wnt inhibitors (*sFRP-1*, *sFRP-2*, *sFRP-3*, *notum*), Wnt-PCP pathways (*DAAM1*, *ROCK*, *vangl2*), and FGFR-like/*nou-darake* family factors (*ndl-3*, *ndl-4*). At least 5 animals were examined in each condition except for *wntP-2*, *DAAM1*, *ROCK*, *vangl2* RNAi treatments in which at least 24 animals were examined. Asterisks indicate $p < 0.05$ from Fisher's exact test versus control + *ptk7* dsRNA treatment after Benjamini-Hochberg correction for false discovery. Inhibition of *ptk7* along with either *wntP-2* ($p=5.16E-14$), *ndl-3* ($p=1.24E-05$), *fzd-1/2/7* ($p=0.046$), or *Dvl-2* ($p=4.18E-06$) caused the strongest occurrence of the ectopic pharynx phenotype. (Lower) in situ hybridizations showing regionalized expression of selected genes from the screen.

DOI: [10.7554/eLife.12850.005](https://doi.org/10.7554/eLife.12850.005)

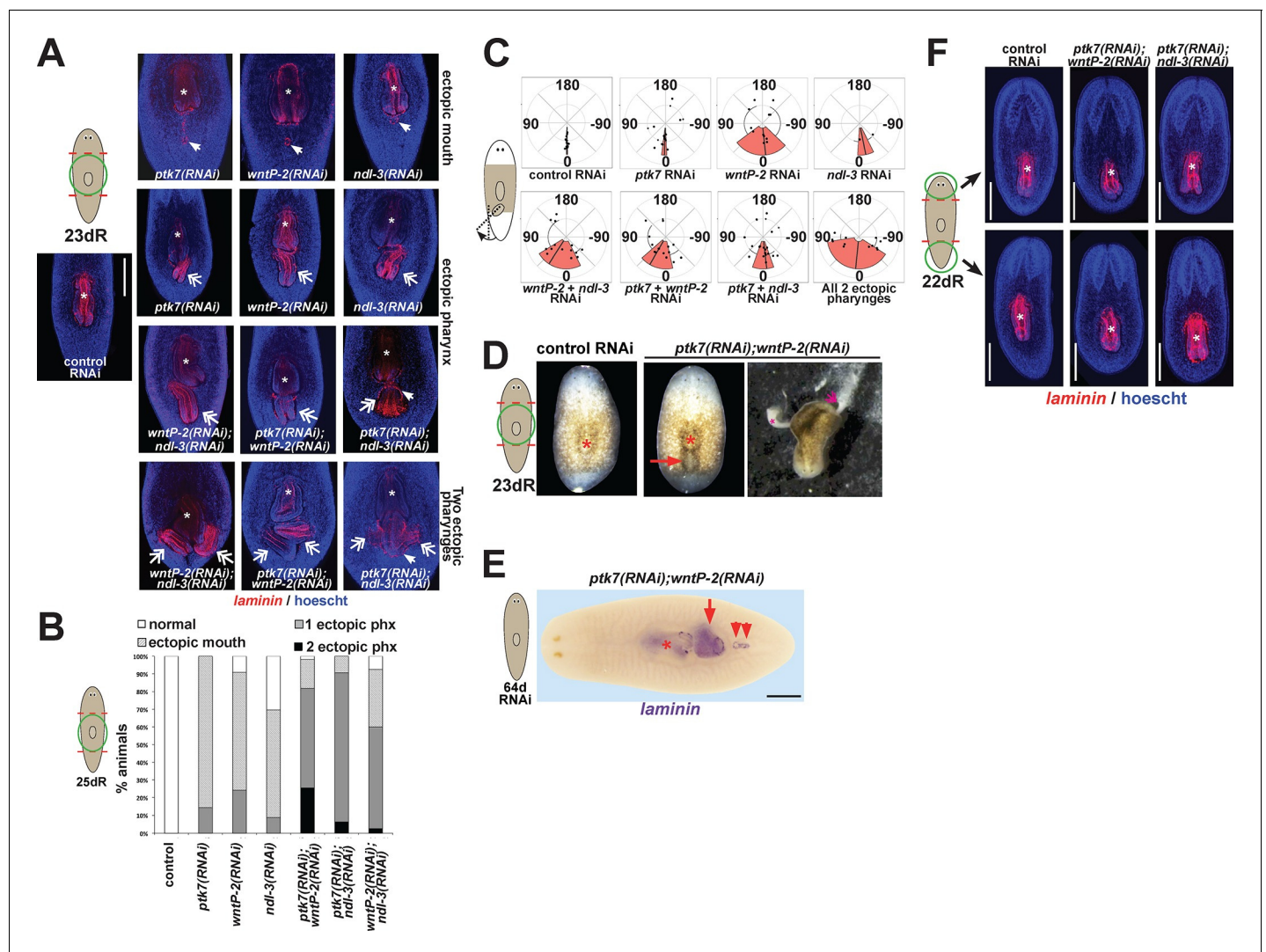


Figure 2. *ptk7* acts with *wntP-2* and *ndl-3* to suppress trunk identity in a context-dependent manner. (A) *ptk7*, *wntP-2*, and *ndl-3* dsRNAs were fed to animals individually or in pair-wise combinations prior to amputation to remove heads and tails, fixation 25 days later, staining with a *laminin* riboprobe and Hoechst dye. (B) Scoring information for pharynx and mouth duplication phenotypes. Animals were scored for presence of ectopic mouth (defined as a superficial circle of *laminin*⁺ cells which was always present posterior to the original mouth, arrow), and ectopic pharynx (defined as having pharynx morphology by *laminin*⁺ and Hoechst⁺ staining, double arrows) and its orientation with respect to the A-P body axis. Animals with an ectopic mouth but not a fully formed ectopic pharynx often had varying degrees of internal *laminin* expression suggestive of a growing pharynx primordium and were scored as having an ectopic mouth only. Co-inhibition of any pairwise combination of the three genes enhanced the penetrance and expressivity of the ectopic pharynx phenotypes. Note that combined pairwise inhibition of *ptk7*, *wntP-2* and *ndl-3* enhanced the trunk duplication phenotype and that dual inhibition of *ptk7* and *wntP-2* produced the strongest effects. (C) Analysis of ectopic pharynx orientation, measured at the proximal end of the ectopic pharynx. In many cases, the ectopic pharynx was oriented at an oblique angle with respect to the body axis, perhaps as a result of ectopic mouth placement nearby the original mouth, and ectopic pharynxes were observed with fully inverted polarity. In all animals that formed 2 ectopic pharynxes (derived from pairwise combinations of dsRNAs), both structures were oriented toward a common ectopic mouth located along the posterior midline. (D) Images of live animals showing the ectopic pharynx in *ptk7*(RNAi);*wntP-2*(RNAi) animals (red arrow) can be functional for feeding. (E) Prolonged inhibition of *ptk7* and *wntP-2* in uninjured animals for at least 36 days (64 days shown) caused formation of an ectopic pharynx (6/8 animals) and multiple posterior mouths (8/8 animals). (F) Inhibition of *ptk7* and *wntP-2* or *ptk7* and *ndl-3* caused head and tail fragments to regenerate only a single pharynx like control animals. Therefore, the effects of *ptk7*, *ndl-3* and *wntP-2* in body patterning are context dependent. Anterior, left. Bars, 300 (A,E) or 500 (F) microns.

DOI: [10.7554/eLife.12850.006](https://doi.org/10.7554/eLife.12850.006)

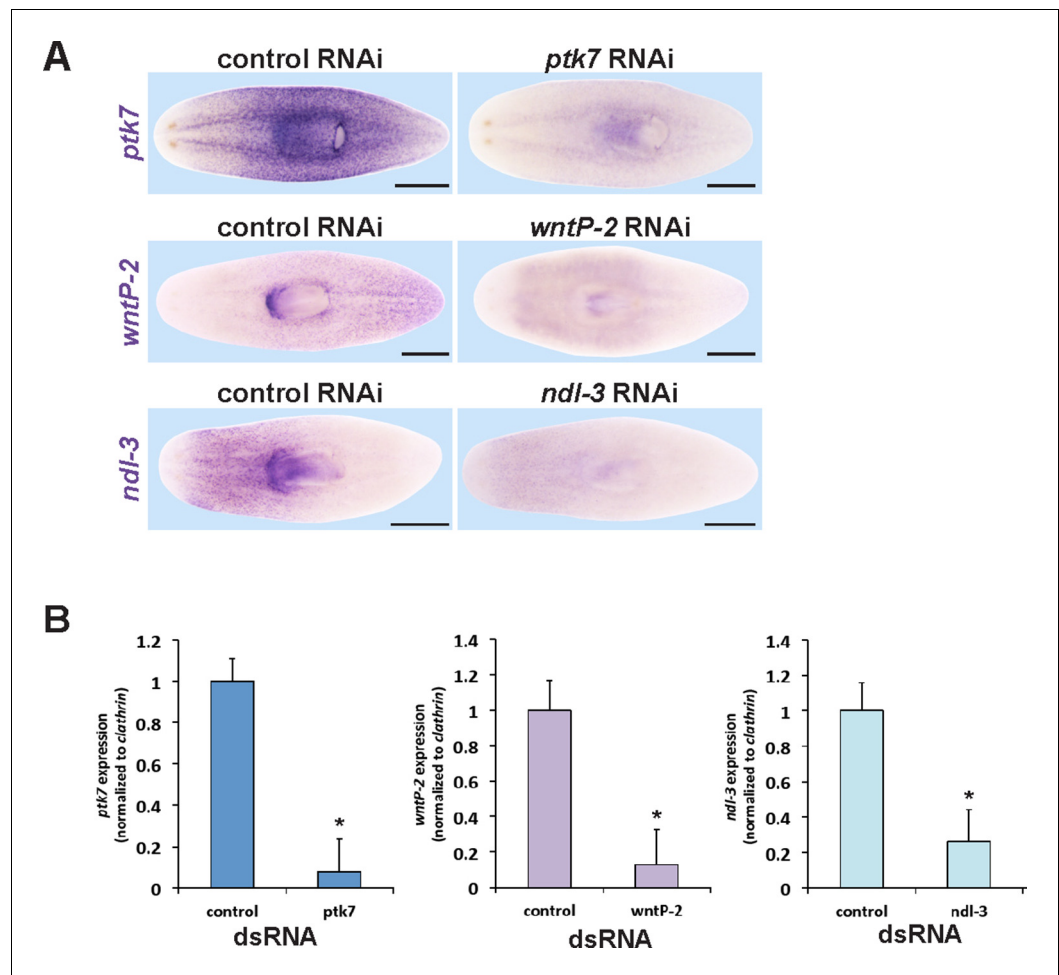


Figure 2—figure supplement 1. Verification of RNAi knockdown for *ptk7*, *wntP-2* and *ndl-3*. (A) In situ hybridizations verifying that dsRNA to *ptk7*, *wntP-2*, and *ndl-3* individually reduced the expression of each gene after 12 days of RNAi in the absence of injury (*ptk7*) or 20 days regeneration after head and tail amputation (*wntP-2* and *ndl-3*) of RNAi. Images represent 100% of animals stained, $n > 4$. Bars, 500 microns. (B) qPCR showing knockdown of *ptk7*, *wntP-2* and *ndl-3* mRNA. Asterisks indicate $p < 0.05$ by a 2-tailed t-test.

DOI: [10.7554/eLife.12850.007](https://doi.org/10.7554/eLife.12850.007)

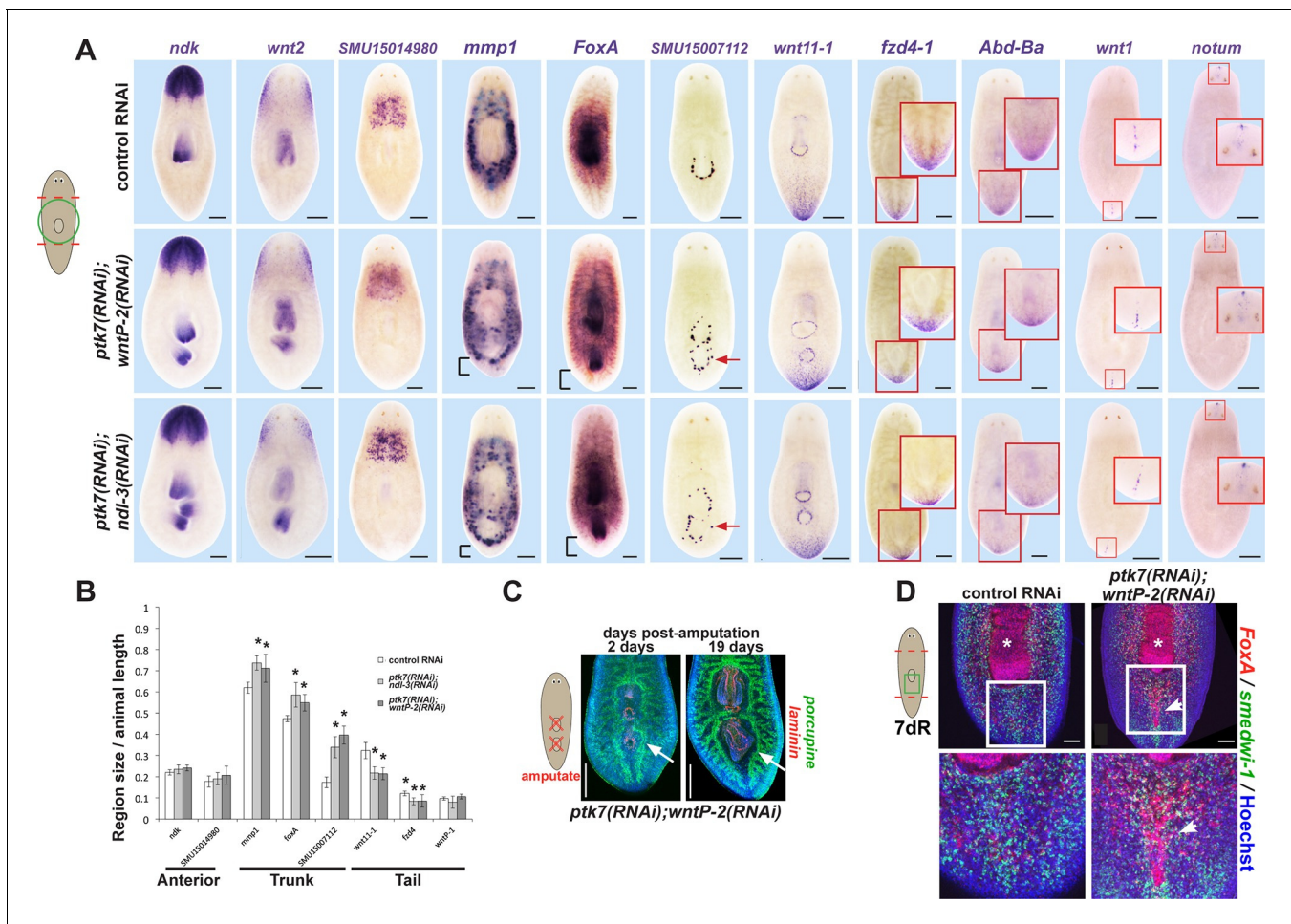


Figure 3. *ptk7*, *wntP-2* and *ndl-3* control tail-versus-trunk identity. (A) In situ hybridizations to detect A-P tissue regionalization in control and *ptk7* (*RNAi*);*wntP-2*(*RNAi*) and *ptk7*(*RNAi*);*ndl-3*(*RNAi*) regenerating trunk fragments fixed 21 days after head and tail amputation, marking the anterior and head region (*ndk*, *wnt2*), prepharyngeal region (novel gene *SMU15014980*), trunk (novel gene *SMU15007112*, *mmp1*, *foxA*), posterior (*wnt11-1*, *fzd4-1*, *Abd-Ba*), and the anterior and posterior poles (*wnt1*, *notum*). All panels represent 100% of at least 6 animals stained. Arrow, ectopic trunk gene expression. Brackets, decrease in size of tail domain. (B) Quantitation of domain size changes from experiments described in (A), measured as length of domain normalized to body length. *ptk7*(*RNAi*);*wntP-2*(*RNAi*) and *ptk7*(*RNAi*);*ndl-3*(*RNAi*) regenerating trunk fragments had increased sizes of trunk domains marked by expression of *mmp1*, *foxA* and *SMU15007112*, and decreased sizes of tail domains marked by expression of *wnt11-1* and *fzd4-1* with little to no change to other domains. Asterisks, $p < 0.05$ by 2-tailed t-test. (C) Both the pre-existing and ectopic pharynx in *wntP-2*(*RNAi*);*ptk7*(*RNAi*) animals regenerated (4/4 animals) after amputation with brief sodium azide treatment, using FISH to mark the gut (*porcupine*, green) and mouth and pharynx (*laminin*, red). Asterisk, pre-existing pharynx; arrows, ectopic pharynx, arrowhead, ectopic mouth. (D) *ptk7*(*RNAi*);*wntP-2*(*RNAi*) animals form ectopic *FoxA*+ cells by day 7 of regeneration. Bars, 100 (D), 200 (A), or 300 (C) microns.

DOI: 10.7554/eLife.12850.009

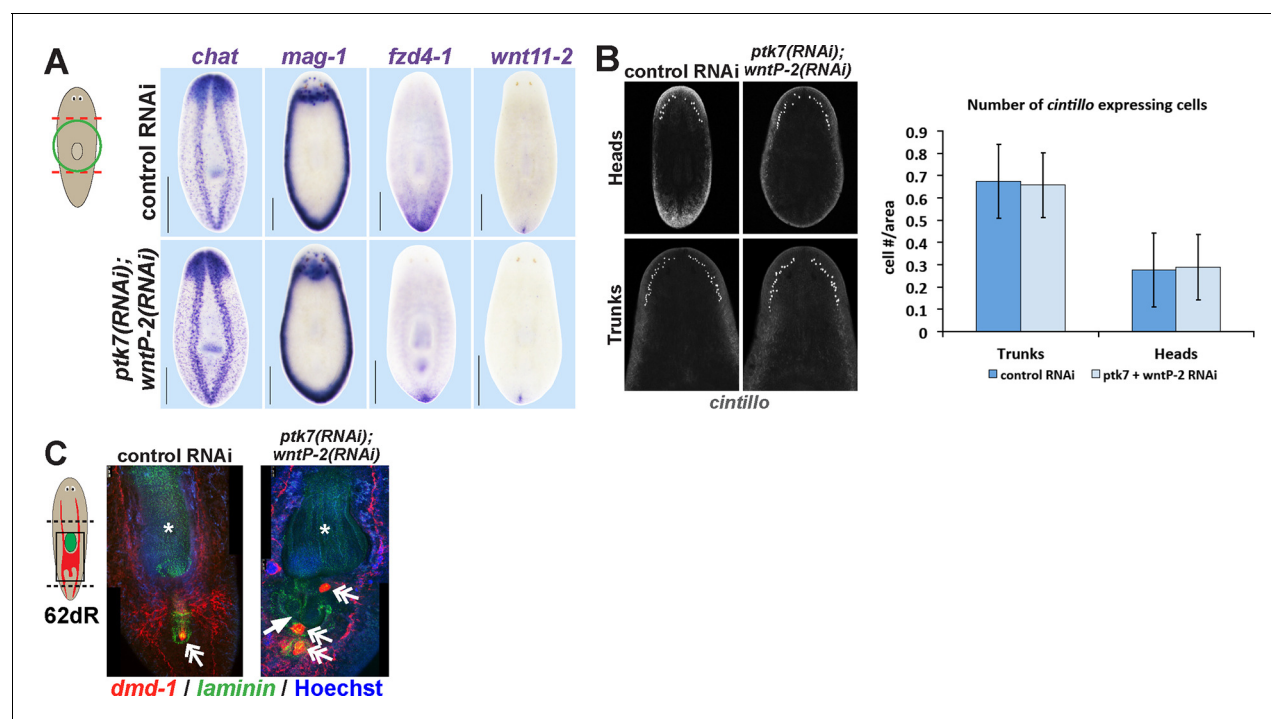


Figure 3—figure supplement 1. Additional histological analysis of *ptk7(RNAi);wntP-2(RNAi)* and animals. (A) In situ hybridizations as in 2A showing normal expression of *chat*, *mag-1*, and *wnt11-2*, but reduced expression domain of *fzd4-1* in *ptk7(RNAi);wntP-2(RNAi)* animals 18 days after head and tail amputation. (B, left) Co-inhibition of *ptk7* and *wntP-2* did not affect numbers of *cintillo*+ neurons of the lateral brain region in day 21 regenerating head fragments or trunk fragments, (B, right) with quantifications of cell number normalized to animal area. Anterior, top. (C) Control sexual strain animals regenerate to have a single pharynx (asterisk, *laminin* expression) and a penis papilla (double arrow, *dmd-1* expression) within the trunk (8/8 animals), whereas *ptk7(RNAi);wntP-2(RNAi)* animals regenerated to form an ectopic *laminin*+ pharynx (arrow, 7/7 animals) and ectopic *dmd-1*-expressing tissues (3/7 animals). Bars, 400 microns.

DOI: [10.7554/eLife.12850.010](https://doi.org/10.7554/eLife.12850.010)

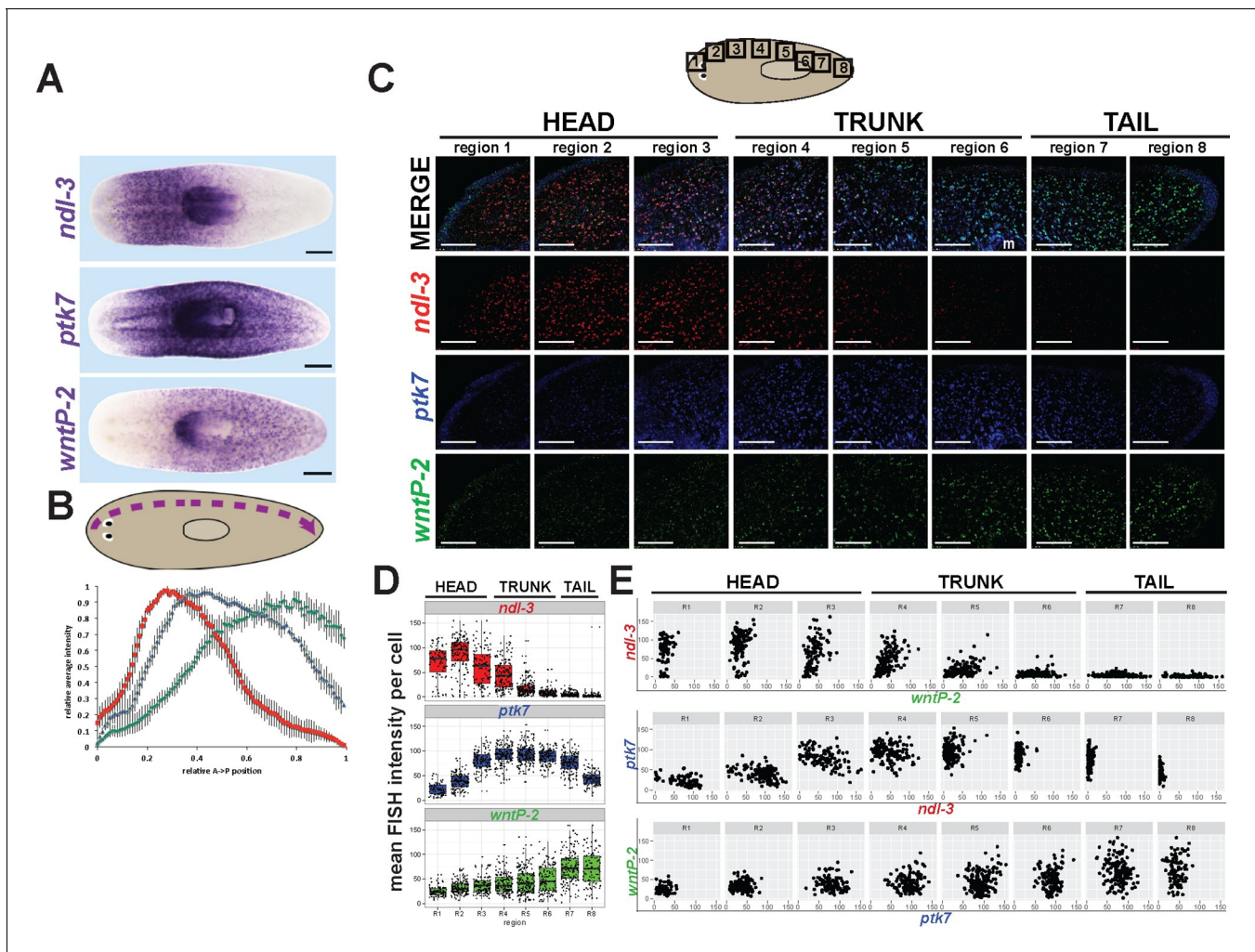


Figure 4. *ndl-3*, *ptk7*, and *wntP-2* are expressed in a graded fashion in domains along the anteroposterior axis. (A) In situ hybridizations showing body-wide graded expression of *ptk7* centered in the trunk, *wntP-2* expression in a gradient from the posterior and *ndl-3* expression in a graded fashion from the anterior. (B) Quantitation of colorimetric in situ hybridization staining across the body axis. 4–6 planarians stained as in (A) were imaged on a dissecting microscope, the images were inverted and then analyzed for position-specific staining intensity along a lateral domain depicted in the diagram (dotted line with arrow showing directionality). To compare animals of different lengths, position was normalized to length of this domain and signal intensity was normalized such that the minimum and maximum values across each animal were 0 and 1, respectively, and average intensity at each region was determined for animals stained with each probe treatment computed followed by obtaining average intensity, with bars showing standard deviations. (C) Triple FISH showing expression of *ndl-3* (red), *ptk7* (blue), and *wntP-2* (green) mRNA. Panels are maximum projections from a stack of seven 1-micron thick confocal images taken at 40x along the body axis at the regions represented in the cartoon, then adjusted for brightness and contrast uniformly for each channel across the image series. m, mouth. Bars, 100 microns. (D–E) Quantification of FISH signal intensity for cells identified in images shown in (C). 3-color images were segmented by merging all three channels to define a set of cells in each region with *wntP-2*, *ndl-3* and/or *ptk7* expression and this mask used to measure mean FISH signal intensity for each cell. (D) Scatter and box plots showing expression of *ndl-3* highest in the anterior, expression of *ptk7* highest in the trunk and tail, and highest *wntP-2* expression in the posterior. (E) Plots comparing pairwise FISH signal intensity between the indicated genes across eight body axis regions (R1–R8) as in (C). Note the existence of cells expressing both *ndl-3* and *wntP-2* (R3–R5), *ptk7* and *ndl-3* (R3–R4), and *wntP-2* and *ptk7* (R5–R7). Bars, 100 (C) or 200 (A) microns.

DOI: 10.7554/eLife.12850.011

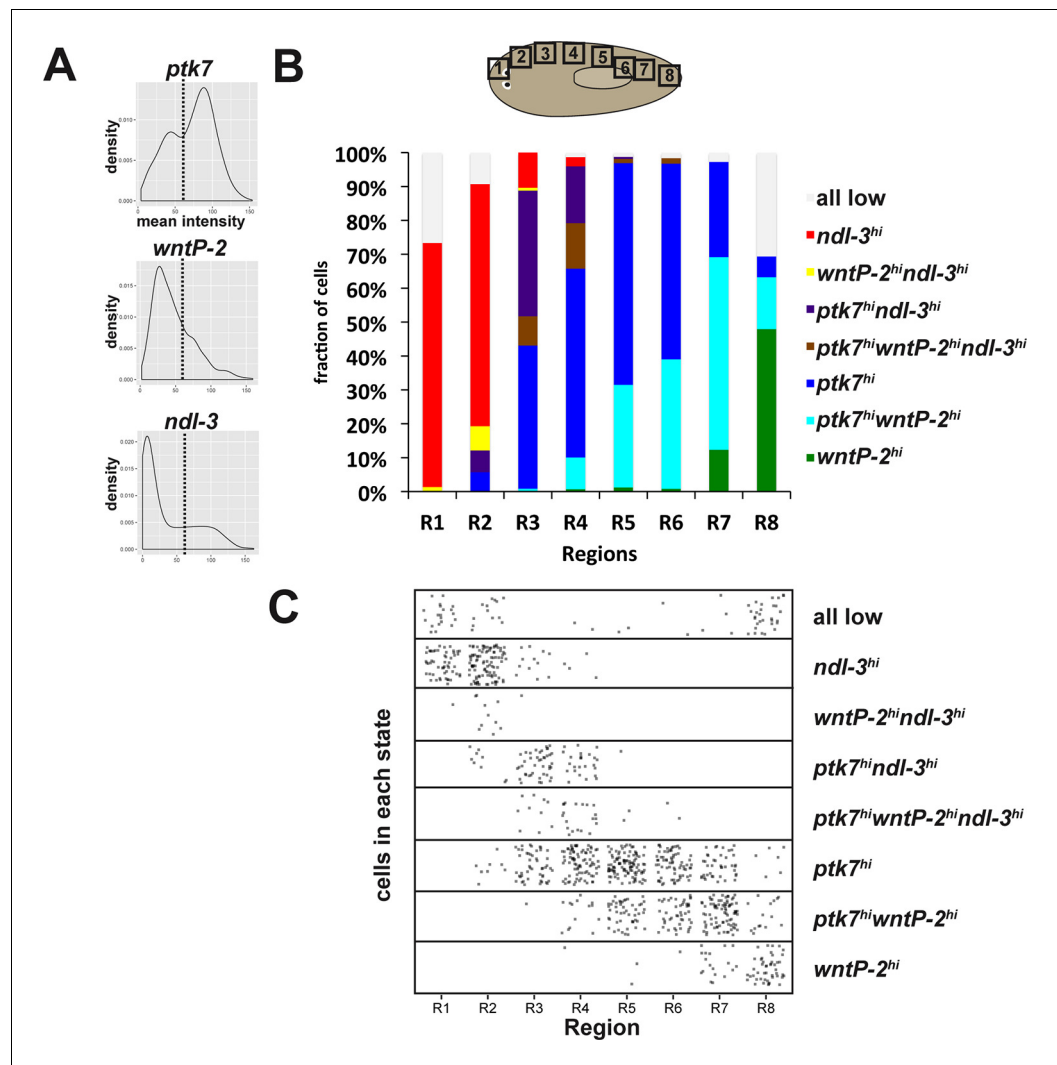


Figure 4—figure supplement 1. Distribution of *ptk7*, *wntP-2* and *ndl-3* expression states across the body axis. (A) Mean fluorescence intensity of cells from all regions in **Figure 4C** were combined and density histograms plotted to determine a cutoff (dotted line=55 in arbitrary units) for higher versus lower expression of *ptk7*, *wntP-2*, and *ndl-3*. Cells within each region shown in **Figure 4C** were assigned membership in one of eight classes defined by high ('hi') or low (unstated) expression of each of the three genes (1: $wntP-2^{hi}$ only, 2: $ptk7^{hi}wntP-2^{hi}$, 3: $ptk7^{hi}$ only, 4: $ptk7^{hi}wntP-2^{hi}ndl-3^{hi}$, 5: $ptk7^{hi}ndl-3^{hi}$, 6: $wntP-2^{hi}ndl-3^{hi}$, 7: $ndl-3^{hi}$, 8: all 3 genes low). Class membership was plotted as a fraction of all cells measured in each region (B) and as a scatterplot of all cells examined (C). By these criteria, several classes of cells expressing combinations of *ptk7*, *wntP-2*, and *ndl-3* exist and are distributed in domains along the body axis. The tail tip has the highest frequency of *wntP-2*+ only cells, whereas anterior tail and trunk regions have a comparatively greater fraction of *wntP-2*+*ptk7*+ cells. The above analysis was repeated for a range of high/low expression cutoffs between 30 and 75, resulting in similar the same trends, with lower thresholds resulting in fewer cells assigned as $ptk7^{lo}wntP-2^{lo}ndl-3^{lo}$ and more cells as $ptk7^{hi}wntP-2^{hi}ndl-3^{hi}$.

DOI: [10.7554/eLife.12850.012](https://doi.org/10.7554/eLife.12850.012)

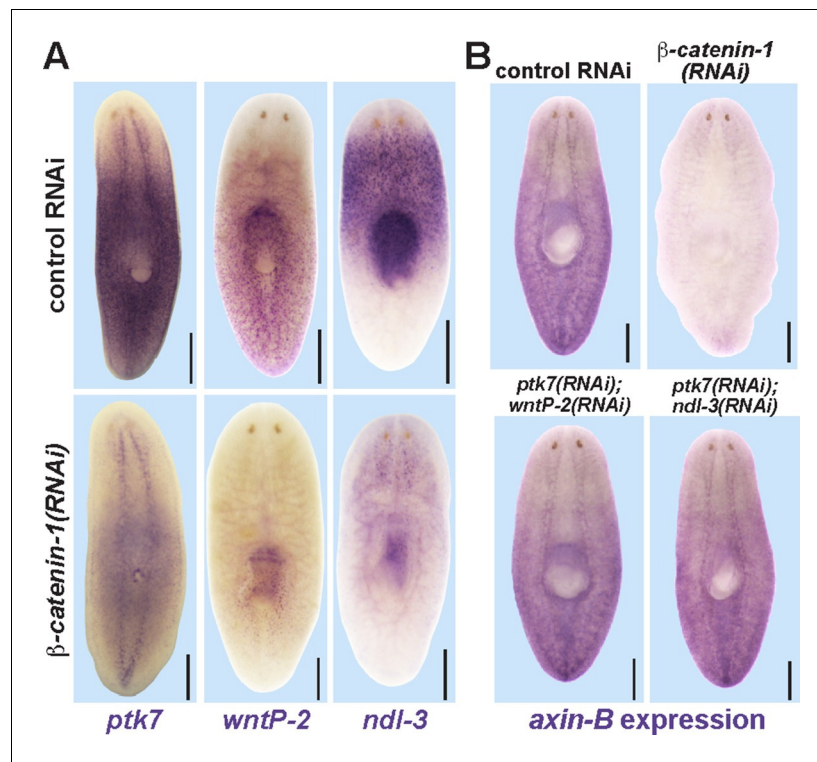


Figure 5. Trunk control genes likely signal independently of β -catenin-1. (A) In situ hybridizations show reduced expression of *ptk7* (11/11 animals), *wntP-2* (6/6 animals), and *ndl-3* (6/6 animals) after 8 days (*wntP-2*, *ndl-3*) or 19 days (*ptk7*) of β -catenin-1 RNAi in uninjured animals. (B) In situ hybridizations showing reduction of *axin-B* expression after 11 days of β -catenin-1 RNAi (14/14 animals) but not after inhibition of *wntP-2* and *ptk7* (14/14 animals) or *ndl-3* and *ptk7* (14/14 animals). Bars, 400 microns.

DOI: [10.7554/eLife.12850.013](https://doi.org/10.7554/eLife.12850.013)

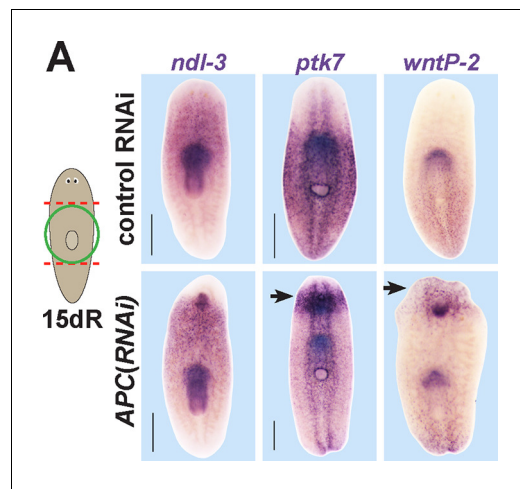


Figure 5—figure supplement 1. Examining the effect of *APC* RNAi on expression of *ptk7*, *wntP-2*, and *ndl-3*. *APC(RNAi)* regenerating animals formed a domain of ectopic *ptk7* (8/8 animals) and *wntP-2* (9/9 animals) expression in the anterior tail. The ectopic tail appears to have a domain expressing *wntP-2* and not *ptk7* at the terminus and a domain expressing both *ptk7* and *wntP-2* near the amputation site. Such animals form an ectopic anterior pharynx likely as the consequence of tail formation, and this expressed *ndl-3*, *ptk7*, and *wntP-2*. Bars, 400 microns.

DOI: [10.7554/eLife.12850.014](https://doi.org/10.7554/eLife.12850.014)

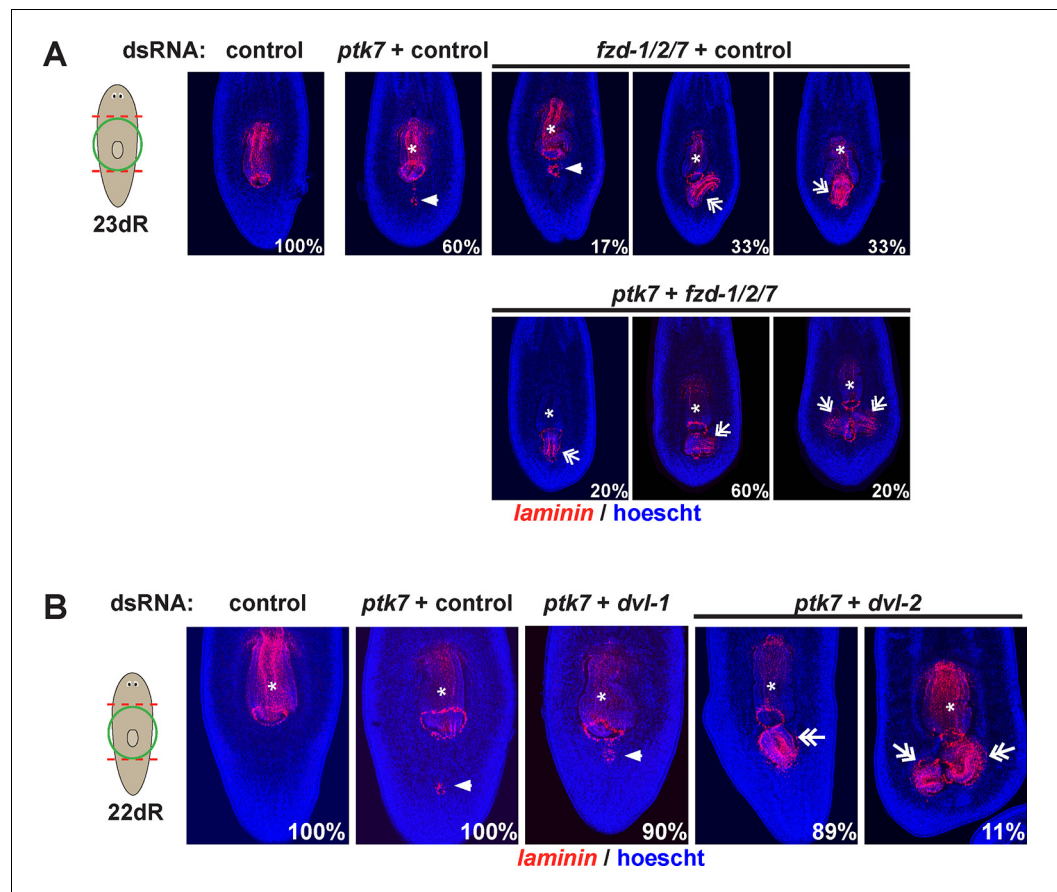


Figure 5—figure supplement 2. *fzd1/2/7* and *dvl-2* inhibition causes ectopic pharynx and mouth formation in the posterior. The indicated dsRNA was delivered to animals by injection prior to amputation, 23 days of regeneration and staining for *laminin* expression to detect pharyngeal tissues. *fzd1/2/7* inhibition (4/6 animals) caused formation of an ectopic pharynx similar to *ptk7*, *wntP-2* and/or *ndl-3* inhibition. *dvl-2* dsRNA enhanced the *ptk7* ectopic pharynx phenotype (9/9 animals). Bars, 300 microns.

DOI: [10.7554/eLife.12850.015](https://doi.org/10.7554/eLife.12850.015)

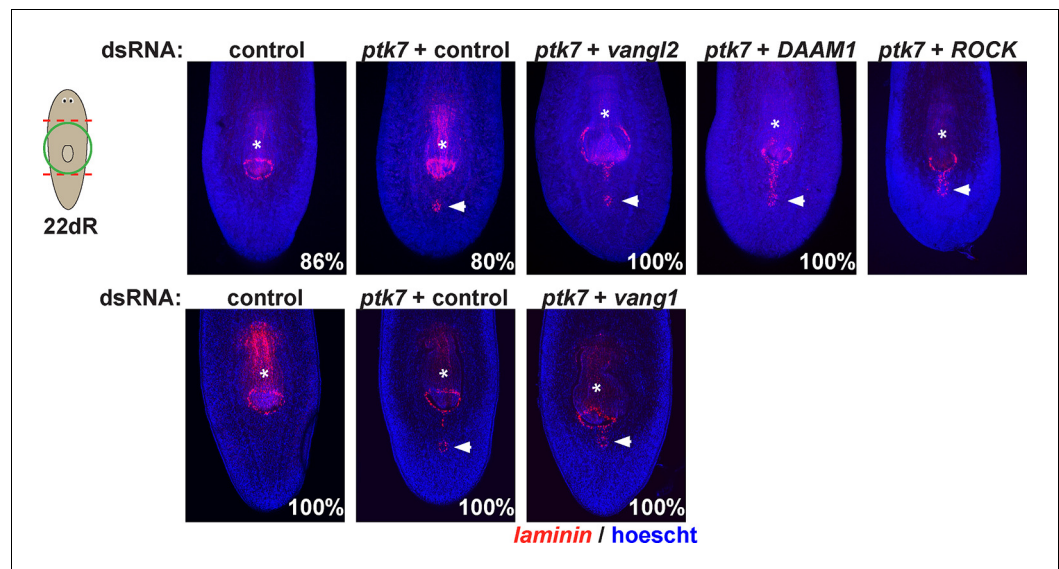


Figure 5—figure supplement 3. Testing planar cell polarity genes for involvement in trunk patterning. Regenerating trunk fragments undergoing RNAi as indicated and stained by FISH with a *laminin* riboprobe to detect the pharynx and mouth. Inhibition of *ptk7* along with *vangl1* (8/8 animals), *vangl2* (4/4 animals), *DAAM1* (6/6 animals) and *ROCK* (6/6 animals) did not suppress or enhance defects due to *ptk7* inhibition alone. Bars, 300 microns.

DOI: [10.7554/eLife.12850.016](https://doi.org/10.7554/eLife.12850.016)

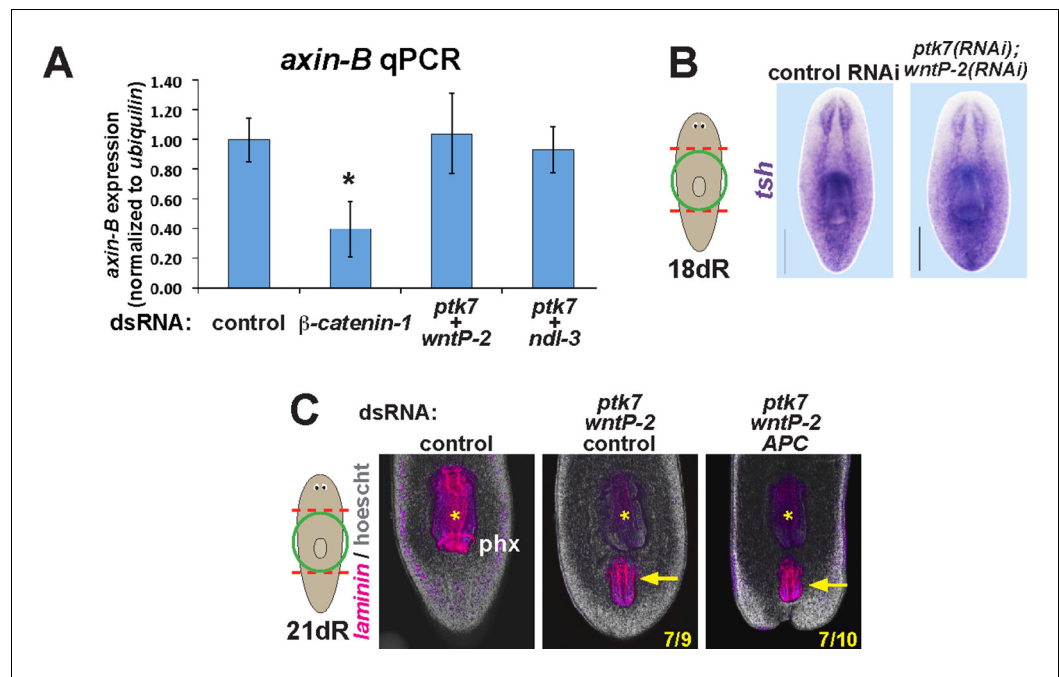


Figure 5—figure supplement 4. *ptk7*, *wntP-2*, and *ndl-3* inhibition do not influence *axin-B* expression and are not modified by APC inhibition. (A) qPCR detecting expression of *axin-B* normalized to *ubiquitin* on RNA purified from day 10 regenerating animals after the indicated dsRNA treatments. β -*catenin-1* inhibition reduced relative *axin-B* mRNA abundance, but *ptk7*+*wntP-2* dsRNA and *ptk7* + *ndl-3* dsRNA had no effect. (B) *ptk7*+ *wntP-2* RNAi did not alter expression of the β -*catenin-1* target gene *teashirt* in animals 18 days after head and tail amputation (3/3 animals). (C) APC inhibition did not detectably affect the frequency of ectopic pharynx formation due to *ptk7* and *wntP-2* RNAi ($p=1.000$, Fisher's exact test) (animals that regenerated an ectopic pharynx: 0/10 control fragments, 0/10 APC(RNAi) fragments, 7/9 *ptk7(RNAi);wntP-2(RNAi);control(RNAi)* fragments and 7/10 *ptk7(RNAi);wntP-2(RNAi);APC(RNAi)* fragments). Bars, 200 microns. Anterior, top.

DOI: [10.7554/eLife.12850.017](https://doi.org/10.7554/eLife.12850.017)

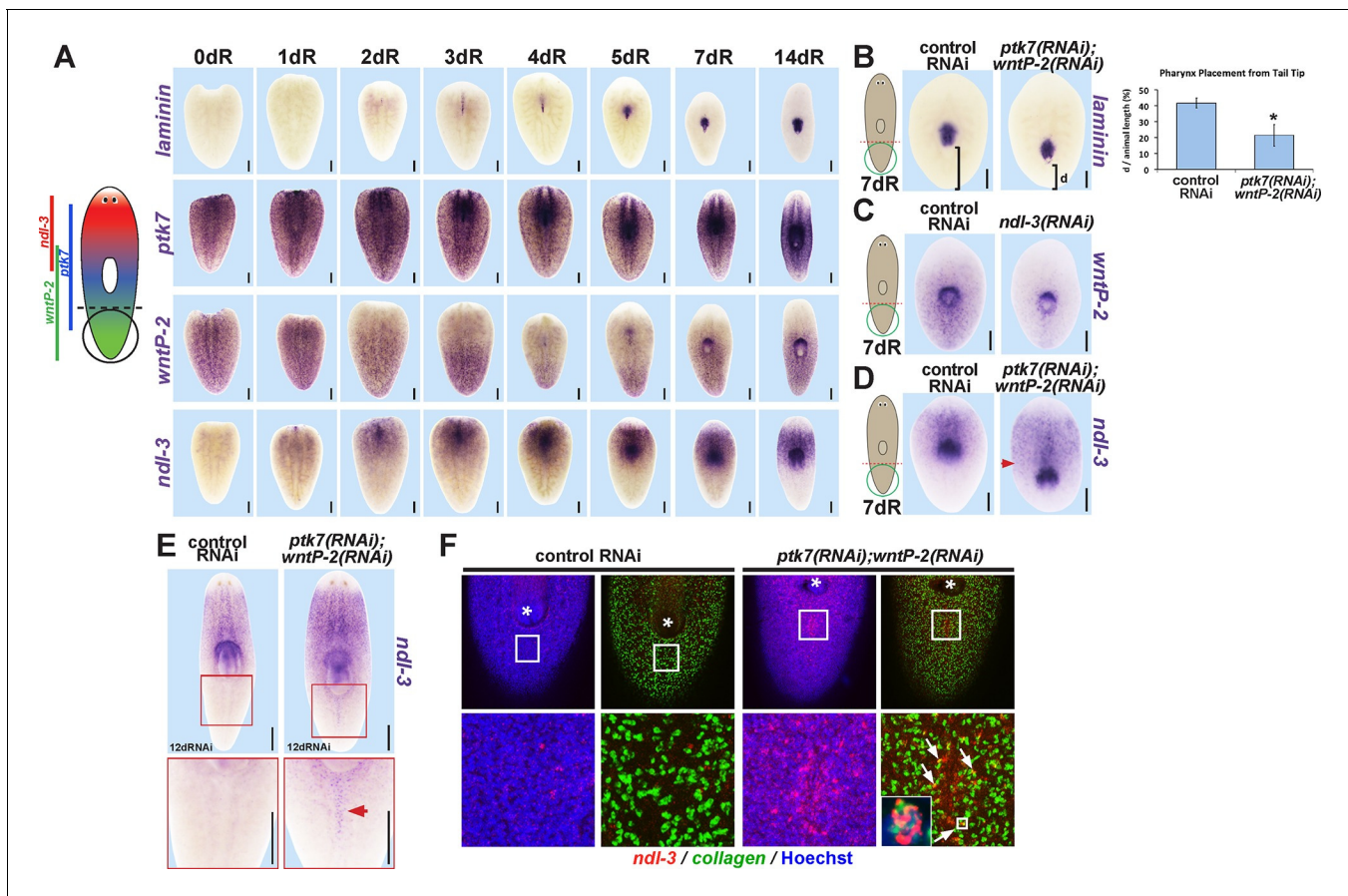


Figure 6. *ptk7* acts with *wntP-2* and *ndl-3* to specify trunk position in regeneration. (A) Cartoon shows regions of trunk control gene expression and in uninjured animals. In situ hybridizations of regenerating tail fragments showing that pharynx formation (marked by *laminin* expression) coincides with early reduction of *wntP-2* expression and increase in *ndl-3* expression. *ptk7* is expressed broadly and re-establishes a trunk-centered gradient by 7 days. All images represent at least 4/4 animals probed except *laminin* (d0) and *ptk7* (d0, d3 and d4) representing 3/3 animals probed. (B) *ptk7(RNAi);wntP-2(RNAi)* animals form a single pharynx located too far posteriorly (7/8 animals, graph shows average distance between posterior pole and *laminin* expression domain normalized to animal length as in **Figure 6—figure supplement 1A–B**, error bars are standard deviations and asterisks shows $p < 0.05$ by a 2-tailed t-test. (C) *wntP-2* expression is reduced in *ndl-3(RNAi)* regenerating tail fragments (10/14 animals). (D–E) *ndl-3* expression is expanded posteriorly in (D) *ptk7(RNAi);wntP-2(RNAi)* regenerating tail fragments by 7 days after amputation (4/5 animals) and in (E) intact animals after 12 or 17 days of RNAi (25/28 animals). (F) Control or *ptk7(RNAi);wntP-2(RNAi)* animals were stained for *ndl-3* and collagen expression after 17 days of RNAi and optical sections were imaged of the body-wall musculature in the region posterior to the pre-existing pharynx. Simultaneous inhibition of *ptk7* and *wntP-2* increased the frequency of *ndl-3+collagen+* cells versus total *ndl-3+* cells found in the tail region (41 of 63 cells in *ptk7(RNAi);wntP-2(RNAi)* animals versus 7 of 32 cells scored in control animals, $p < 0.0001$ by Fisher's exact test). Bars, 200 (A–D) or 400 (E) microns.

DOI: [10.7554/eLife.12850.018](https://doi.org/10.7554/eLife.12850.018)

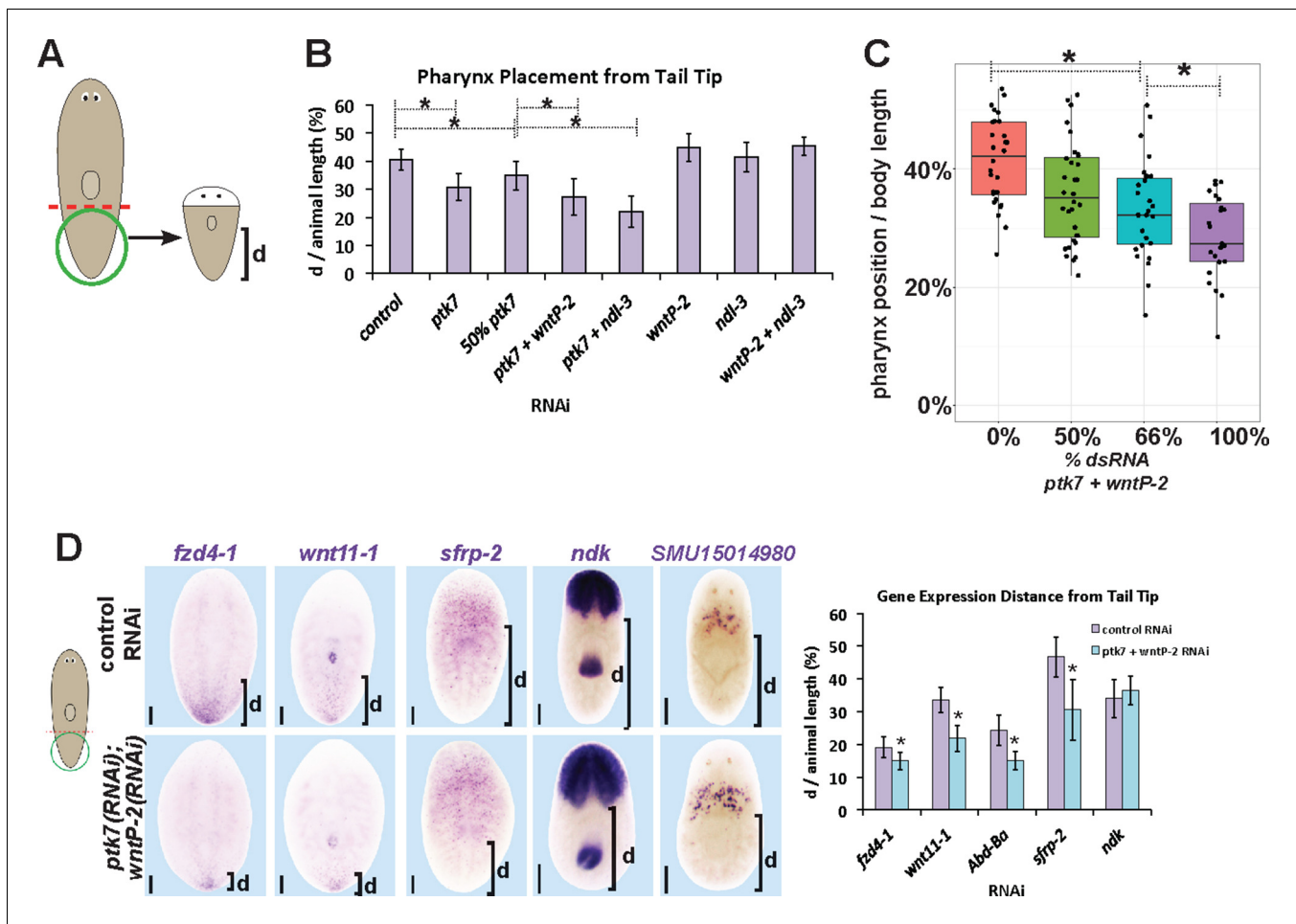


Figure 6—figure supplement 1. *ptk7*, *wntP-2* and *ndl-3* participate in positioning the pharynx during tail fragment regeneration. (A) Assay design used to measure pharynx position in (B–C). **Figure 4B** (B) Quantification of pharynx placement phenotypes in 7 day regenerating tail fragments after inhibition of *wntP-2*, *ptk7* and *ndl-3* singly or in pairwise combinations as indicated. The strongest effects were observed after simultaneous inhibition of *ptk7* and *wntP-2* or *ptk7* and *ndl-3*. Bars, averages; asterisks indicate $p < 0.05$ by 2-tailed t-test. (C) Dilution of *ptk7*+*wntP-2* dsRNA with control dsRNA caused a progressively weaker pharynx placement phenotype, suggesting a gradation of their activities affect trunk position. (D, left) *ptk7(RNAi); wntP-2(RNAi)* animals stained with riboprobes to several regionally expressed genes shows such animals form normal anterior and prepharyngeal regions, but have posteriorly shifted trunk and tail gene expression domains quantified in (D, right). Graphs show averages of at least 7 samples, error bars show standard deviations, and asterisks indicate $p < 0.05$ by two-tailed t-test. Bars, 200 microns.

DOI: [10.7554/eLife.12850.019](https://doi.org/10.7554/eLife.12850.019)

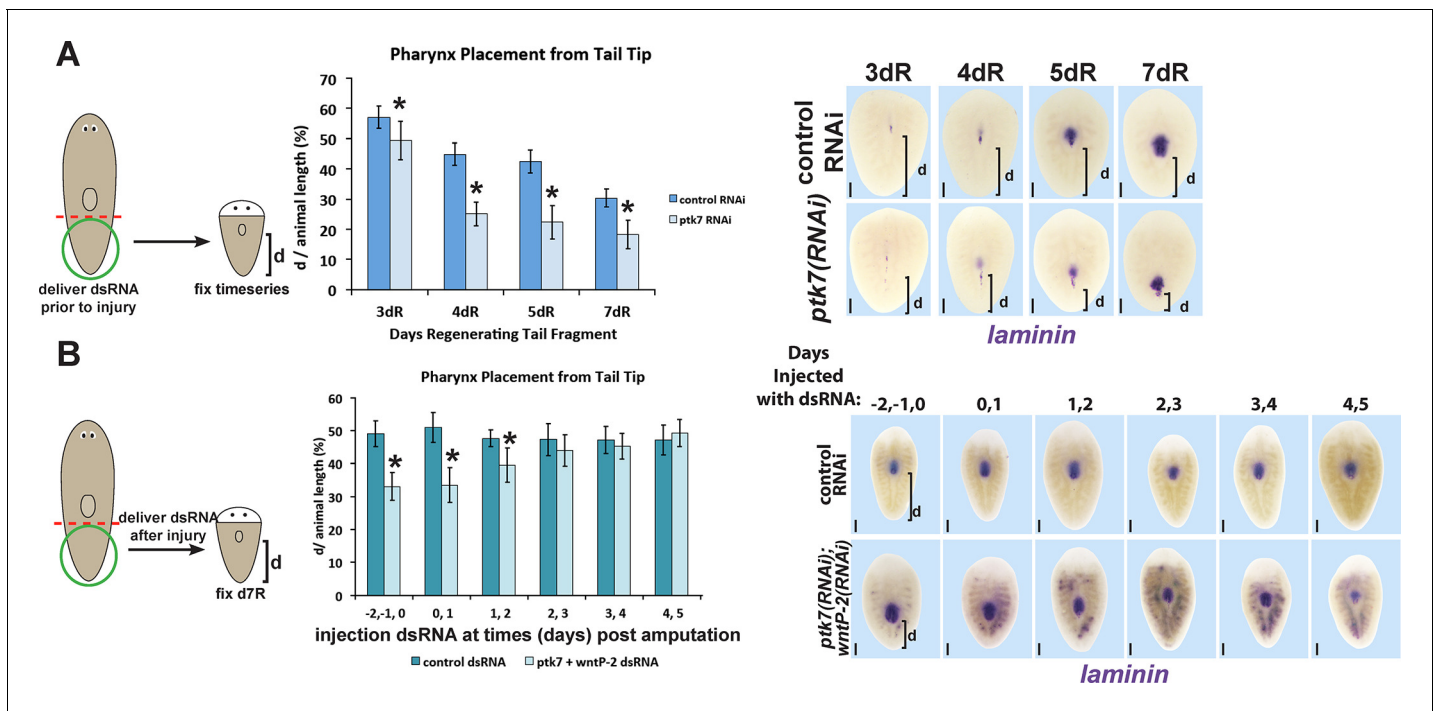


Figure 6—figure supplement 2. Determining critical period for *ptk7*/*wntP-2* signaling in pharynx placement. (A) Measurements of pharynx position as in **Figure 4—figure supplement 1A** at selected days after amputation in regenerating control or *ptk7*(RNAi) regenerating tail fragments treated with dsRNA for three days prior to amputation or (B) injected with control or both *wntP-2* and *ptk7* dsRNA only at the indicated days with respect to the day of amputation (day 0). Injection of *wntP-2*+*ptk7* dsRNA as late as 1–2 days after amputation can posteriorize the position of the regenerated pharynx. Graphs show averages of at least 4 samples, error bars show standard deviations, and asterisks indicate $p < 0.05$ by two-tailed t-test. Bars, 200 microns.

DOI: [10.7554/eLife.12850.020](https://doi.org/10.7554/eLife.12850.020)

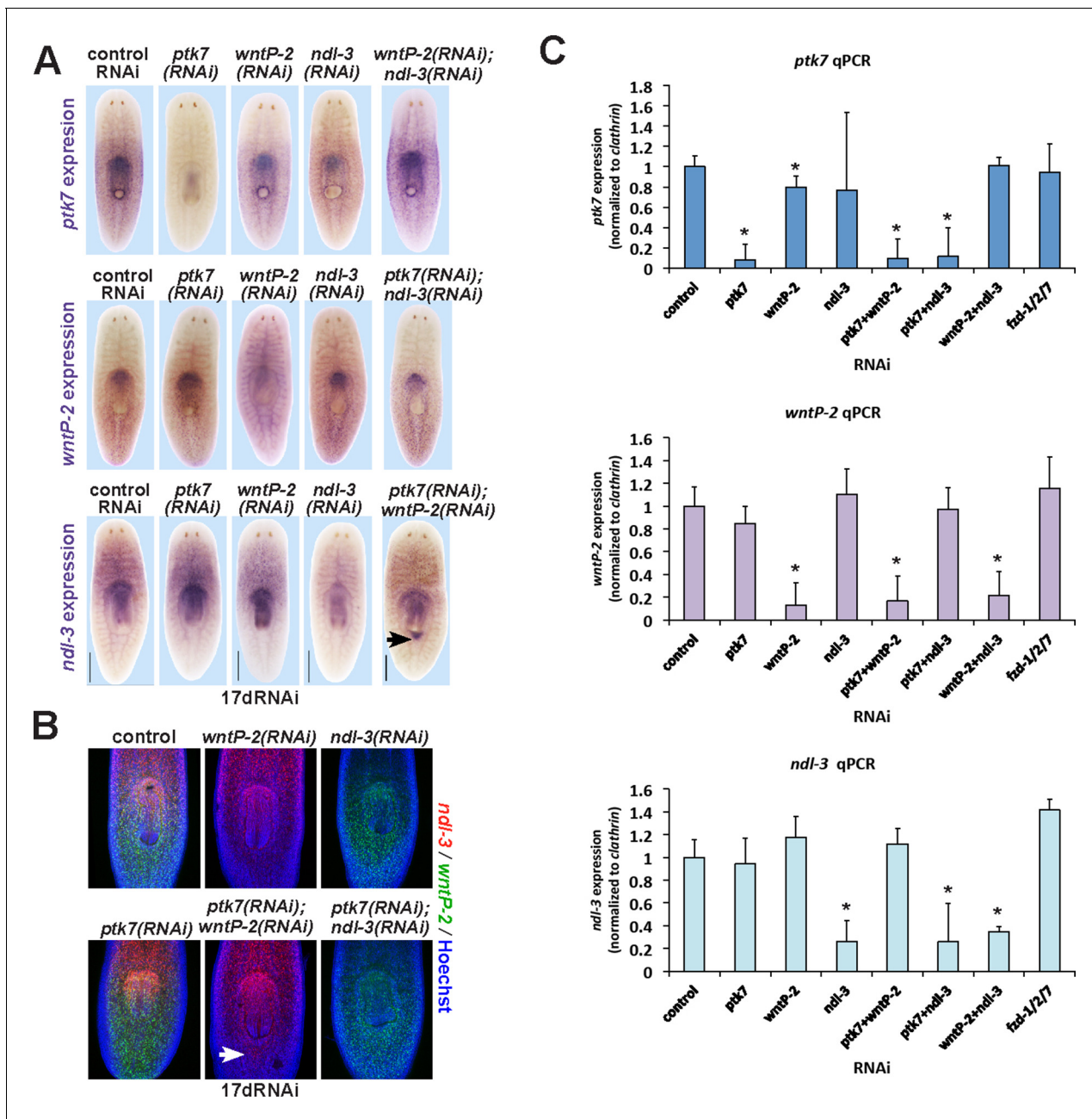


Figure 6—figure supplement 3. Examining the influence of *ptk7*, *wntP-2* and *ndl-3* on each other's expression. (A–C) Examining intact animals for regulatory interactions among trunk control genes. Uninjured animals fed with the indicated dsRNAs for two weeks prior to fixation and staining by (A) WISH or (B) FISH to examine effects on expression of *ptk7*, *wntP-2* or *ndl-3*. No treatment caused strongly increased or reduced expression except for *ptk7*+*wntP-2* RNAi which caused ectopic expression of *ndl-3* in the anterior tail region (A, 5/8 animals; B, 12/15 animals). (C) Animals were treated with dsRNA as in A and B, then analyzed by qPCR for expression changes to *ptk7*, *wntP-2*, and *ndl-3* following RNAi. Inhibition of each gene caused similar knockdown in either single or double-RNAi contexts. *wntP-2* RNAi caused a weak but statistically significant reduction to *ptk7* transcript levels, similar to WISH detection (A). *fzd-1/2/7* RNAi did not significantly alter expression of *ptk7*, *wntP-2*, or *ndl-3*. Bars, 400 microns (A), 300 microns (B).

DOI: 10.7554/eLife.12850.021

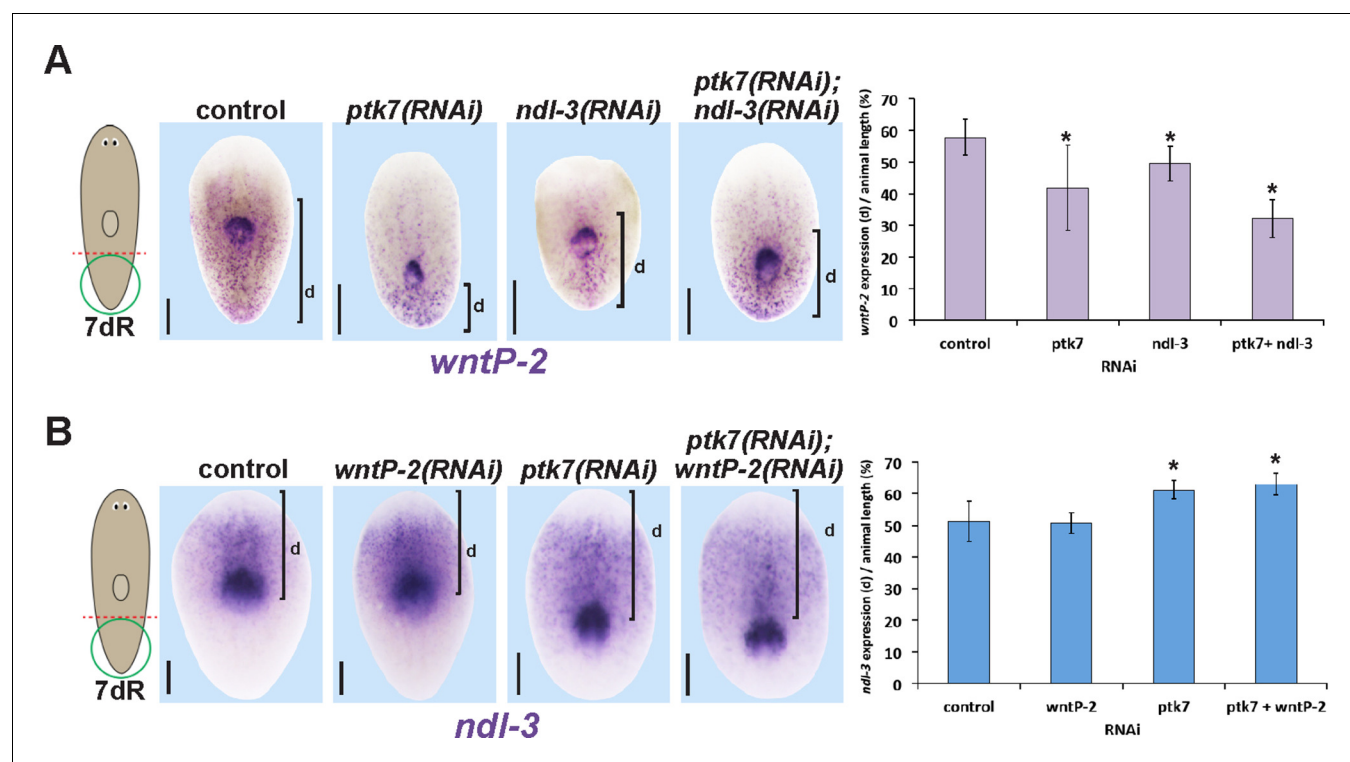


Figure 6—figure supplement 4. Measurements of the influence of trunk control genes on *wntP-2* and *ndl-3* expression in tail fragment regeneration. (A–B) Animals were treated with the indicated dsRNAs for three days prior to amputation, regenerating tail fragments were fixed 7 days later, and stained for (A) *wntP-2* expression or (B) *ndl-3* expression. Measurements were made from the posterior tip of the regenerating animal to (A) the anterior edge of *wntP-2* expression or (B) the posterior edge of *ndl-3* expression then normalized to animal length. Graphs show averages and error bars are standard deviations. Asterisks indicate $p < 0.05$ by a 2-tailed t-test. Bars, 200 microns.

DOI: [10.7554/eLife.12850.022](https://doi.org/10.7554/eLife.12850.022)

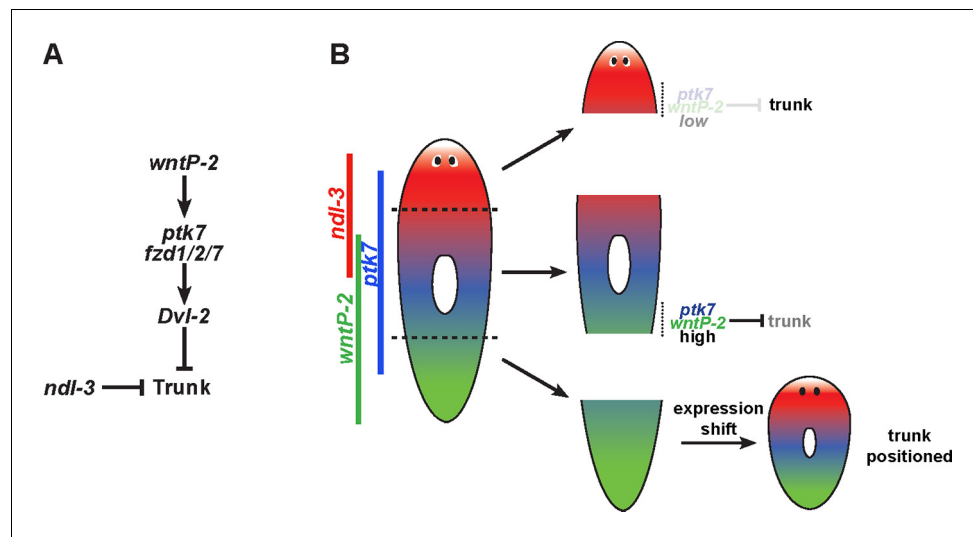


Figure 7. Model for *wntP-2*, *ptk7* and *ndl-3* in control of patterning. **(A)** A candidate molecular pathway of action in which *wntP-2* signals through *ptk7* and *fzd1/2/7* and *Dvl-2* to suppress trunk identity within the anterior tail region. The FGFRL *ndl-3* acts with the same sign as these components to suppress trunk regionalization and could act in a parallel pathway or modify the activity of the pathway through an unknown mechanism. *wntP-2* and *ptk7* can inhibit *ndl-3* expression in the posterior of regenerating tail fragments and intact animals and *ndl-3* promotes *wntP-2* expression in regenerating tail fragments, suggesting the potential for feedback regulation within this pathway (not shown). β -catenin-1 signaling is required upstream for expression of *ptk7*, *wntP-2* and *ndl-3* (not shown). **(B)** Model relating expression of pathway components to patterning functions. The highest region of expression co-expression of *wntP-2* and *ptk7* occurs in the anterior tail and trunk at a location where these genes prevent trunk fates in animals undergoing tissue homeostatic maintenance and in regenerating trunk fragments that form new tail tissues. By contrast, regenerating head fragments lack abundant co-expression of *wntP-2* and *ptk7*, which we suggest is important for enabling the normal formation of trunk regional identity and regeneration of associated structures. Regenerating tail fragments would initially possess high levels of *wntP-2* and *ptk7* predicted to suppress trunk identity, but undergo a regeneration expression regulatory program that reduces *wntP-2* mRNA in this region, enabling trunk regeneration at a position that we suggest could be defined by a particular A-P location of *ptk7* and *wntP-2* activity present at an appropriate time in regeneration. According to this model, *wntP-2/ptk7* signaling provides information about the presence/absence of the trunk region used to control regeneration outcomes.

DOI: [10.7554/eLife.12850.023](https://doi.org/10.7554/eLife.12850.023)